Characterization of Semicrystalline Polymers by Inverse Gas Chromatography. 1. Poly(vinylidene fluoride)

Chein-Tai Chen and Zeki Y. Al-Saigh*

Department of Chemistry, University of Charleston, 2300 MacCorkle Avenue, SE, Charleston, West Virginia 25304. *Received May 2, 1988; Revised Manuscript Received December 20, 1988*

ABSTRACT: Inverse gas chromatography as a method for polymer characterization was applied to poly(vinylidene fluoride) (PVF2) below and above its melting temperature. Twenty low molecular weight solutes (probes) were used in this study. A retention diagram for PVF2 was obtained that showed a change in the thermal isotherm in the region below melting temperature. The retention volumes of 20 probes showed dependence on the solid support, the carrier-gas flow rate, and the loading of PVF2. A procedure was developed and discussed to correct for all of these effects and to calculate meaningful solute-retention volumes related only to the solute sorption in the amorphous part, thus eliminating the contribution of V_g to the adsorption of solutes on the crystalline and amorphous surfaces. The Flory–Huggins interaction parameters χ_{12} for all probes below PVF2 melting temperature and for alkanes above PVF2 melting temperatures were calculated and discussed. The percent crystallinity of PVF2 was calculated in the temperature range 80–160 °C: a range of 64–29% was obtained. The crystallinity data were incorporated to calculate the specific volume of PVF2 below its melting temperature (80–160 °C). The IGC method provided data on the partial molar sorption as well as mixing functions of solutes in molten and crystalline PVF2, below and above its melting temperature. These thermodynamic data were discussed with respect to the contribution of methyl groups in alkanes and acetates and the carbonyl group in acetates to the PVF2 backbone site–solute. Acetates are found to be good solvents for PVF2 and show negative heats of mixing, while alkanes were found to be nonsolvents for PVF2 (positive heats of mixing). Our calculation showed that methyl groups interact stronger than carbonyl groups with PVF2 backbone sites.

Introduction

It has been shown that inverse gas chromatography (IGC) can be an accurate, reliable, and fast method of obtaining physicochemical properties of polymers and polymer blends and of the structure and chemical interactions of macromolecules.[1-11] The term "inverse" indicates that the polymeric stationary phase of the chromatographic column is of interest in contrast to the conventional gas chromatography experiments. A wealth of thermodynamic data can be obtained by applying the IGC method to polymer–solvent systems: solubility parameters, interaction parameters, diffusion constants, enthalpies of mixing, surface areas, adsorption isotherm, glass transition temperatures, melting temperatures, and degree of crystallinity.

In our ongoing research on the IGC method and its application to polymer–solvent and polymer–polymer systems,[1] we have improved the experimental precision by correcting for many experimental effects: the contribution of the solid support to the retention volume,[1] the effect of the carrier-gas flow rate, the effect of the polymer loading,[2] and the effect of the volume of the probe injected on the retention volume. The foregoing effects were not fully recognized by previous researchers. Most recently, we obtained a precise measurement of the probe retention time by fully automating our system using a personal computer and an analog-to-digital convertor. Utilizing correction procedures for these effects in this work, we will show that meaningful values for the specific retention volumes (V_g) and semicrystalline polymer–solute interaction parameters χ_{12}, specific volumes, and degree of crystallinity were obtained using high molecular weight semicrystalline poly(vinylidene fluoride). We found that the following steps are satisfactory in our corrections: (1) A soaking method for coating the polymer on the solid support, developed by Al-Saigh and Munk,[1] is used in this work for a better control of the mass of the polymer. (2) The apparent retention volumes of the probes were corrected for the solid support contribution. (3) The retention volumes data were extrapolated to zero flow rate of the carrier gas to compensate for slow establishment of the phase equilibrium.[8,12] (4) The corrected retention volumes were then extrapolated to infinite loading of the polymer to eliminate the effect of the probe adsorption on the surface of the polymer. Applying these corrections on the retention volumes of solutes with a different chemical nature with PVF2 gave our data, in this report, reliable precision.

Smidsrod and Guillet were pioneers in examining the retention diagram of amorphous polymers.[3] They found that the nature of such a retention diagram depends strongly on the probe used. They divided the retention diagram into three isotherms: equilibrium surface adsorption, nonequilibrium sorption, and equilibrium sorption. For semicrystalline polymers, the retention diagram has an additional phase transition in the nonequilibrium region just below the melting temperature.[3,13,14] Few data are available on semicrystalline polymers particularly below the melting temperature because the retention mechanism is more complicated than that in the amorphous polymers.

There has been an increasing interest in PVF2 as it is often used in many applications such as in electronic industries. PVF2 is a highly polar polymer that possesses ferroelectrical (piezoelectrical and pyroelectrical) properties,[15] and it has an interesting lattice complexity. Because IGC has not been fully applied on semicrystalline polymers, we decided to characterize PVF2 using the IGC method below and above its melting temperature. It is our hope, in this paper, that data obtained with the IGC method could be used to explain the physicochemical properties of PVF2 below and above its melting temperature.

Data Reductions

The probe-specific retention volumes V_g corrected to 0 °C were calculated from the standard chromatographic relation:[15]

$$V_g^0 = \frac{273.15 \Delta t F J}{w T_{room}} \quad (1)$$

where $\Delta t = t_p - t_m$ is the difference between the retention

* To whom all correspondence should be addressed.

0024-9297/89/2222-2974$01.50/0

time of the probe t_p and the marker t_m. F is the flow rate of the carrier gas measured at room temperature T_{room}, w is the mass of the polymeric stationary phase, and J is a correction factor for gas compressibility defined by the following relation:

$$J = \frac{3}{2}\frac{(P_i/P_o)^2 - 1}{(P_i/P_o)^3 - 1} \quad (2)$$

where P_i and P_o are the inlet and outlet pressures, respectively.

The PVF2–solute interaction parameters at infinite dilution of the different solutes used in this work are defined by the following:

$$\chi_{12} = \ln \frac{273.15Rv_2}{V_g^0 P_1^0 V_1} - 1 + \frac{V_1}{M_2 v_2} - \frac{(B_{11} - V_1)}{RT}P_1^0$$

or

$$\chi_{12} = \ln \frac{273.15Rv_2}{V_g^0 V_1 P_1^0} - 1 - \frac{P_1^0}{RT}(B_{11} - V_1) \quad (3)$$

where R has the usual meaning as the gas constant, V_g is the specific retention volume of PVF2 in mL/g, V_1 is the molar volume of the solute, P_1^0 is the vapor pressure, M_2 is the molecular weight of the polymer, and B_{11} is the second virial coefficient of the solute in the gaseous state. It should be noted that specific volume, V_1, P_1^0, and B_{11} were calculated at the column temperature. Since M_2 is a large term, the term V_1/M_2 becomes negligible. We will refer to the solute by the subscript 1 and PVF2 by the subscript 2.

The vapor pressures P_1^0 were calculated from the Antoine equation as follows:

$$\log P_1^0 = A - B/(t + C) \quad (4)$$

where t is the temperature in °C, and the constants A, B, and C are taken from Dreisbach's compilation.[17] The molar volumes of the solutes V_1 were calculated by using eq 5–7, where ρ_L and ρ_V are the densities of the liquid

$$V_1 = M_1/\rho_L \quad (5)$$

$$\rho_L + \rho_V = a - bt \quad (6)$$

$$\rho_V = P_1^0 M_1/RT \quad (7)$$

solute and its saturated vapor, respectively, M_1 is the molecular weight of the solute, and P_1^0 is the pressure calculated from eq 4. The constants a and b are also taken from Dreisbach's compilation.[17] Second virial coefficients B_{11} were computed by using[18]

$$B_{11}/V_c = 0.430 - 0.886(T_c/T) - 0.694(T_c/T)^2 - 0.0375(n - 1)(T_c/T)^{4.5} \quad (8)$$

where V_c and T_c are the critical molar volume and the critical temperature of the solute, respectively, and n is the number of carbon atoms in alkane solutes or the number of corresponding groups in nonalkane solutes.

The specific volumes of PVF2 (as the inverse of ρ_{sc}) in the temperature range used in this work were calculated from

$$\rho_{sc}/\rho_a = 1 + 0.13X_c$$

$$\rho_{sc} = 1.74(1 + 0.13X_c) \quad (9)$$

where ρ_{sc} and ρ_a are the densities of semicrystalline and amorphous states of PVF2, and X_c is the degree of the crystallinity of PVF2 as obtained in this work and listed in Table III. The density of the amorphous PVF2 is 1.74 g/mL and was taken as a standard value from ref 19. Table II shows the calculated specific volumes of PVF2 in the temperature range 80–160 °C.

The molar heat (enthalpy) of sorption of probe absorbed by the amorphous part of PVF2 (ΔH_1^s) is given by[20]

$$\Delta H_1^s = -R\delta \ln V_{g_b}^0/\delta(1/T) \quad (10)$$

where V_{g_b} is the net specific retention volume corrected for the flow rate and loadings dependence. By using V_{g_b} in eq 10, we eliminated the contribution of the molar heat of the probe adsorbed on the crystalline and the amorphous surfaces. T is the column temperature.

The average partial molar heat of mixing at infinite dilution of the probe at 473.15 K was calculated as follows:

$$\Delta \bar{H}_1^\infty = R\delta \ln \Omega_1^\infty/\delta(1/T) \quad (11)$$

where Ω_1^∞ is the weight fraction activity coefficient of the solute probe at infinite dilution, which is calculated according to

$$\Omega_1^\infty = \frac{273.15R}{V_g^0 P_1^0 M_1} \exp[-P_1^0(B_{11} - V_1)]RT \quad (12)$$

where P_1^0, V_1, and B_{11} were defined in eq 3, and M_1 is the molecular weight of the probe. Equation 12 was developed by Patterson et al.[21] to replace the original equation for infinite dilution activity coefficient developed by Everett.[22] The original equation depended on an uncertain quantity, i.e., the molecular weight of the polymer.

The partial molar free energy of mixing at infinite dilution is calculated from the weight fraction activity coefficient of the solute as follows:

$$\Delta G_1^\infty = RT \ln \Omega_1^\infty \quad (13)$$

where RT has the usual meaning.

The partial molar free energy of sorption at infinite dilution is calculated as follows:

$$\Delta G_1^s = RT \ln [M_1 V_{g_b}^0/273.15R] \quad (14)$$

By incorporating eq 10 and 14, we calculated the entropy of sorption of solutes as follows:

$$\Delta G_1^s = \Delta H_1^s - T\Delta S_1^s \quad (15)$$

Experimental Section

Materials. Twenty polar and nonpolar probes were used in this study. They were selected to provide several groups of a chemically different nature. They all were purchased from Aldrich Chemical as chromatographic grade, their purity being checked by gas chromatography prior to use. Poly(vinylidene fluoride) (PVF2) was supplied by Aldrich Chemical in powder form. Its molecular weight was measured as M_w = 250 000 by using the GPC technique.[23] Chromosorb W (AW-DMCS treated, 60/80 mesh) was obtained from Analabs.

Instrumentation and Procedure. Measurements were run on a modified Varian 1800 Aerograph gas chromatograph equipped with both thermal conductivity (TC) and flame ionization detectors. The thermal conductivity detector was selected over a flame ionization detector for reasons related to the improvement of the measurements precision in IGC experiments. Using the TC detector, we were able to monitor the carrier-gas flow rate every hour and over a period of 7 h/day without disturbing the flow of the carrier gas. Another advantage of using the TC detector was the use of air as a inert marker to account for the dead volume in the column, thus improving the precision of retention time measurements because a mixture of air and the probe can be injected for each independent experiment. Methane has been used by many IGC researchers in the past. From our experience, it does interact with the stationary phase, and thus correction for methane is deemed necessary. Figure 1 shows a schematic diagram of the experimental setup used in this work.

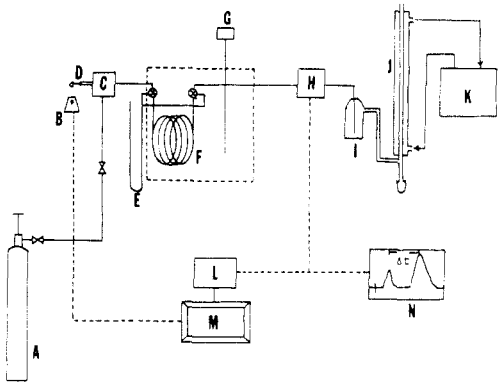

Figure 1. Schematic diagram of automated system for inverse gas chromatography: A, carrier gas; B, microsoft mouse; C, injection port; D, microsyringe; E, manometer; F, column; G, temperature indicator; H, detector; I, Dewar flask; J, bubble flow meter; K, ultrathermostat; L, Chrom-1 interface; M, personal computer; N, strip chart recorder.

Table I
Stationary Phase and Column Descriptions

column	PVF2 loading %, w/w	wt of polym, g	wt of support, g	column length, cm
I	0	0	7.9670	152.4
II	3	0.2399	7.9970	152.4
III	7	0.5631	8.0010	152.4
IV	12	0.9600	7.9950	152.4

Dried nitrogen gas (research grade) was used as a carrier gas; its flow rate was controlled by a series of valves, among them a precision needle valve to ensure stability of the flow. The flow rate was measured by a soap bubble flow meter with a 50-mL volume thermostated at 25 °C. The three readings usually taken agreed well to within 0.3%. A flow rate within a range of 1–30 mL/min was used to explore its influence on V_g values. The inlet and the outlet pressures were frequently monitored (every hour) by a precision mercury manometer. The outlet pressure turned out to be always atmospheric while the inlet pressure ranged around 900 mmHg. The temperature of the column was monitored frequently within the range of 0.1 °C by using a high-precision temperature control and digital indicator (Omega Model DP 701). Control of the mass of the polymer in the stationary phase has been under debate.[24-26] Recently, we developed, with excellent precision, a soaking type method for coating the polymer on the support.[1]

Four columns were prepared with 5-ft-long copper tubing, $^1/_4$-in. o.d. The copper tubings were washed with methanol and were annealed prior to use. Table I shows the description of these columns. Four loading of PVF2 were used ranging from 0 to 12% by weight of the polymer relative to the weight of the solid support. PVF2 was dissolved in hot *N,N*-dimethylformamide (DMF) solution and deposited onto the solid support. Columns were conditioned at 80 °C and fast carrier gas flow rate for 24 h prior to use. Probes were injected onto the columns with 1-μL Hamilton syringes. Three consecutive injections were made for each probe at each set of measurements. An injection volume of 0.2 μL was selected so as to remain within a safe region with minimum effect on the retention volumes. We observed a change in retention volumes with the amount of the probe injected. We followed the method developed by Munk et al.[9] to determine the safe region in which the retention volumes of probes did not change significantly with the volume of the injection. The safe region, however, has to be determined experimentally because it differs from one detector to another and it depends on the type of detector used. The retention times of the probes were measured with high precision as the peak maxima. An analog-to-digital convertor (Chrom-1, Metrabyte) was interfaced with an IBM-compatible personal computer for the detection and integration of the chromatographic signal, which was analyzed as a function of time. The PC was used to control the operation, store the data, display the elution curves, and to perform extensive calculations using the stored data. The whole process was fully automated and controlled by a program developed by Munk and El-Hibri at the University of Texas at Austin, starting from the sample injection to the final retention volume calculations. The measured retention volumes of 20 probes used in this work for the zero loading column (support only) were stored in a separate file and interpolated over a wide range of temperatures. The stored retention volumes of probes were then subtracted from the raw retention volumes of the probes by using other columns with different loadings. This procedure was used to correct for the "inert" solid support effect. Our data handling system saved us a tremendous amount of time in data acquisition and calculations and offered a precision and reproducible results of ±0.1 s in the retention time.

Results and Discussion

Specific Retention Volumes. The specific retention volumes (V_g) of 20 probes with different chemical natures were obtained by using four columns with different loadings of PVF2, 0%, 3%, 7%, and 12%. Experiments were performed below the PVF2 melting temperature at 80, 100, 120, 140, and 160 °C and above the melting temperature at 180, 200, and 220 °C. The probes retention volume was first measured at 80 °C, and the column temperature was systematically increased toward the higher temperatures. The column oven was in a continuous operation from the beginning of the work to the end. This procedure was adopted to prevent any recrystallization and change in the morphology of PVF2 upon the cooling of the column. PVF2 is a semicrystalline polymer in which the spherulitic crystalline regions are embedded in the amorphous matrix. Above the glass transition temperature, probes penetrate around the crystallites and dissolve only in the amorphous portion of PVF2. In this work, we noticed a reduction in the retention volume as compared to that measured with amorphous PVF2 above the melting temperature. This reduction is attributed to the reduced interaction of the probe with the crystalline part of PVF2. Probes have not enough time to penetrate through the crystalline region and therefore their retention is reduced. Because of this structure complexity, PVF2 has at least two retention mechanisms below the melting temperature: surface adsorption and bulk absorption. These mechanisms can be easily explained by means of Martin's equation:[6,27]

$$V_g = K_s(S/W) + K_b \qquad (16)$$

where K_s is the partition coefficient due to surface adsorption, K_b is the partition coefficient due to the bulk absorption, S is the available surface area of the polymeric coating, and w is the mass of the polymer. Because V_g is sensitive to the surface area of the polymer, we used three different loading of PVF2. For a fixed temperature K_s and K_b are constant; therefore, the retention volume will decrease as the loading, w, is increased. Indeed it was the case in this work; we observed a decrease in V_g as w increases for all probes, and we extrapolated all V_g data to infinite loading of PVF2. This step was done after the correction of V_g for the effects of the support and flow rate.

To have a better understanding of the two retention mechanisms, we eliminated the contribution of the solid support to V_g (see the Experimental Section). Independent experiments were performed at three different flow rates using a column packed with only solid support (Figure 2). Specific retention volumes of all probes were corrected for this effect by subtraction of V_g of all probes from the crude (apparent) V_g values from use of columns having three different loadings at three different flow rates and at all temperatures. The corrected V_g values obtained by using this correction differed 10–30% from the apparent V_g values below the PVF2 melting point and 5% from the apparent V_g values above the PVF2 melting point. This

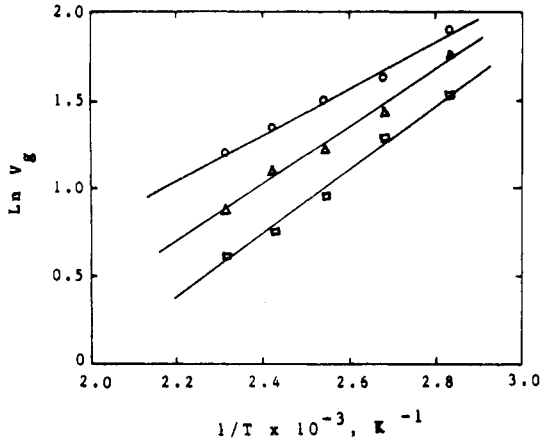

Figure 2. Dependence of the carrier-gas flow rate on the retention volume of *n*-butyl acetate using Chromosorb W at various temperatures: ○, slow (8 mL/min); △, medium (15 mL/min); □, fast (25 mL/min).

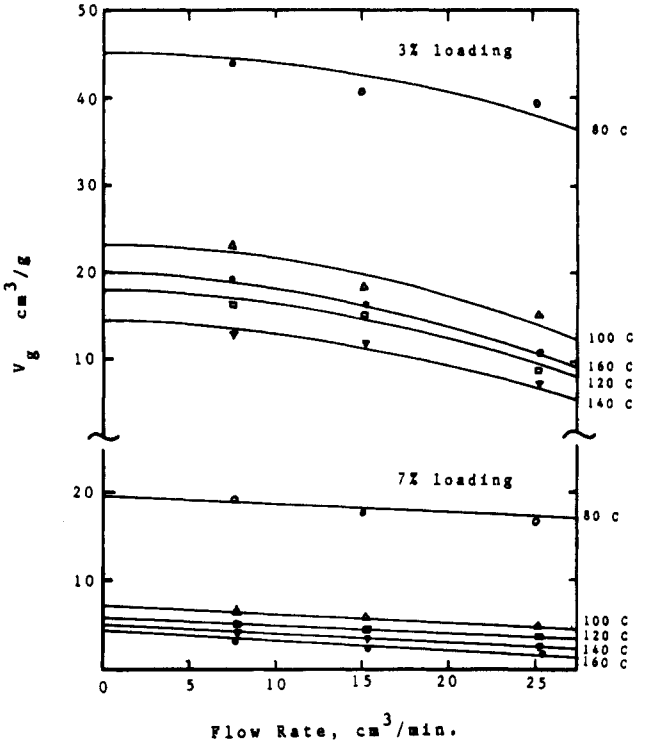

Figure 3. Dependence of the carrier-gas flow rate on the retention volumes of undecane at 3% and 7% of PVF2.

percent error was decreased as the temperature increased. El-Hibri and Munk[28] reported a 10% error for the contribution of the solid support using amorphous polymers. Our result showed a higher percentage contribution of the solid support below the PVF2 melting point, because our V_g values for the semicrystalline polymer are lower than the V_g values for the amorphous polymer. After performance of this correction, V_g data below PVF2 melting of all probes were corrected for the effect of the carrier-gas flow rate. We used three flow rates: slow, 8 mL/min; medium, 15 mL/min; fast, 25 mL/min. V_g data for all probes and at a temperature range of 80–220 °C were plotted vs the flow rate and were extrapolated to zero flow rate. Most of the plots exhibited a decrease of V_g values as the flow rate increased; the decrease was not linear. Tangents for the curves were drawn and extrapolated to zero flow rate; V_g data at the intersection of tangents with the Y axis are considered to be the corrected V_g values for the support and the flow-rate effects. Figure 3 shows a typical plot of V_g values vs flow rate for undecane for 3% and 7% loadings of PVF2. All V_g values were shown to be flow-rate dependent and with an error as high as 50% below the PVF2 melting point and less than 15% above the PVF2 melting point. This error depended on the loading of PVF2, the degree of crystallinity of the polymer, and the temperature of the column. It is clear that slow flow rates (0–5 mL/min) are useful in obtaining reliable V_g values. According to these findings, a flow rate of 4 mL/min is recommended for our future experiments using PVF2. This observation does not agree with Galin and Maslinko,[29] who reported no dependence of flow rate (8–30 mL/min) on V_g values using PVF2 above the melting temperature.

Table II
Specific Volumes of PVF2

temp, °C	percent crystallinity	specific vol, mL/g
80	64.10	0.5305
100	60.30	0.5329
120	55.90	0.5358
140	51.50	0.5387
160	28.70	0.5540
≥180	0.00	0.5750

Table III
Degree of Crystallinity of PVF2 below the Melting Temperature[a]

solute	80 °C	100 °C	120 °C	140 °C	160 °C
methyl acetate	65.70	62.10	59.80	56.40	30.30
ethyl acetate	61.30	57.30	53.20	50.40	28.20
propyl acetate	65.10	60.90	55.50	50.30	27.40
n-butyl acetate	64.30	60.80	55.20	48.80	28.90
average	64.10	60.30	55.90	51.50	28.70

[a] These measurements are based on the retention volumes of the acetate series.

The final correction of V_g values, for all probes and at all temperatures, is for the dependence on PVF2 loadings. Three columns were prepared with 3%, 7%, and 12% of PVF2. The corrected V_g values for the support and flow rate were plotted vs the inverse of loadings. Figures 4 and 5 are typical plots of V_g vs the reciprocal of loading of undecane and propyl acetate at various temperatures. Twenty plots, such as in Figures 4 and 5, for all probes were generated and extrapolated to the infinite loading of PVF2. The V_g values were decreased as the loading increased as predicted in eq 16 in a nonlinear relationship. The curved lines were extrapolated, and their intercept with the Y axis is considered as the corrected V_g values. As is clearly seen from Figures 4 and 5, that loading effect could have contributed to a major error in V_g values. After the performance of these corrections, we believe that the error in the corrected V_g values is less than 2%, thus making the V_g values reliable and meaningful for thermodynamic interpretation. Volatile probes such as pentane, hexane, heptane, and chlorinated hydrocarbons were not used above the PVF2 melting point as our experiments indicate that their retention is very close to the marker retention.

By performing the above procedure, we eliminated the kinetic effect for the slow diffusion of the probe and the contribution of V_g to the surface adsorption. In our case, there are two surface adsorption mechanisms: adsorption on the crystalline surfaces, and adsorption on the amorphous layer surfaces. Thus, our corrected V_g is further treated to include only the mass of the amorphous part of PVF2. This procedure was done by subtracting the mass of the crystalline part of PVF2, using the percentage crystallinity values listed in Table III, from the corrected V_g values. Actually, our final V_g values are the specific retention volume of the probe absorbed by the amorphous

Table IV
Corrected Specific Retention Volumes (V_{g_b}) on PVF2 at Various Temperatures

probe	80 °C	100 °C	120 °C	140 °C	160 °C	180 °C	200 °C	220 °C
pentane	3.19	2.39	1.56	1.15	1.29			
hexane	2.81	2.32	1.99	1.46	1.02			
heptane	4.12	3.29	2.61	1.88	1.15			
octane	5.35	4.01	3.19	2.04	1.25	1.42	1.27	1.12
nonane	7.19	5.06	3.81	2.08	1.39	2.51	1.97	1.81
decane	11.75	7.83	5.31	2.54	1.42	3.59	2.89	2.69
undecane	29.28	8.89	7.62	3.63	2.86	4.85	3.78	3.29
dodecane	35.09	14.61	12.47	4.19	6.34	5.53	4.31	3.82
benzene	14.79	11.89	9.73	6.97	4.61			
toluene	35.82	22.95	15.85	12.08	7.64			
methylene chloride	0.53	0.86	1.16	1.22	0.94			
carbon tetrachloride	4.93	4.18	3.49	2.82	1.79			
tetrahydrofuran	27.02	20.65	15.65	13.19	7.99			
dioxane	120.89	75.82	45.81	29.69	15.57			
acetone	46.52	31.23	19.49	15.46	8.89			
methyl ethyl ketone	60.45	37.28	22.91	18.96	11.78			
methyl acetate	32.59	19.65	13.38	8.87	6.89	4.76	3.53	2.56
ethyl acetate	51.14	31.23	19.73	11.96	8.84	6.62	4.81	3.11
propyl acetate	67.66	43.58	27.35	18.78	12.34	9.11	6.26	4.16
n-butyl acetate	107.16	64.99	39.91	28.02	16.97	12.54	8.43	5.74

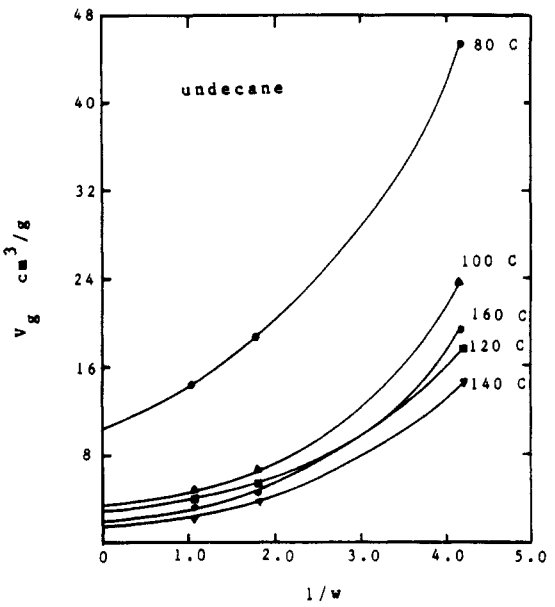

Figure 4. Dependence of PVF2 loadings on the retention volumes of undecane.

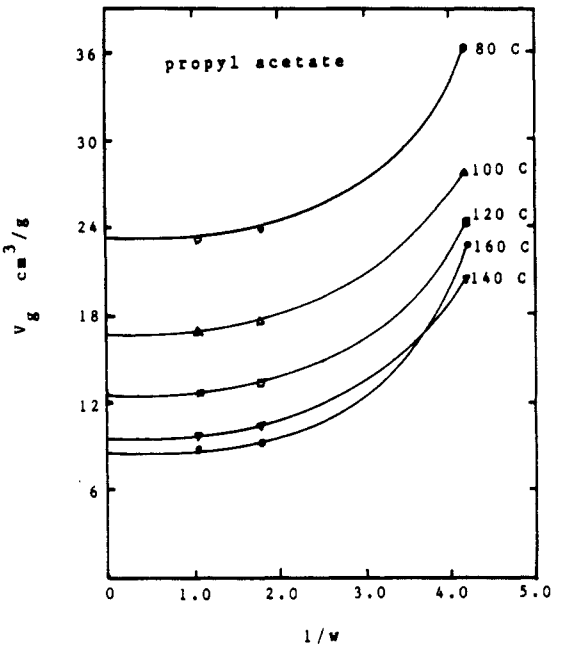

Figure 5. Dependence of PVF2 loadings on the retention volumes of propyl acetate.

part of PVF2 (V_{g_b}). As far as we know, this is the first procedure to be reported for obtaining a meaningful specific retention volumes using semicrystalline polymer. V_{g_b} can be obtained by using

$$V_g^0 = \frac{273.15\Delta t F J}{w(1 - X_c)T_{room}} \quad (17)$$

Table IV shows V_{g_b} values for 20 probes and at various temperatures. These values indicate that carbonyl-containing compounds including acetates and dioxane have more interaction with PVF2 than other solvents used in this work. Alkanes are poor solvents for PVF2 while acetates, ketones, and dioxane are good solvents for PVF2. The interaction of these probes showed a significant dependence on the chemical nature of the probe and temperature.

The net retention volumes of 20 probes, corrected for the flow rate and loadings, were plotted against the inverse of temperature. They all showed a linear relationship between 80 and 140 °C, with different slopes. The slopes of the retention curve for alkanes showed an increase with number of carbons in the series; it was less pronounced in the case of acetates. A pronounced curving up break was observed between 140 and 160 °C, above which a straight line was observed. Figure 6 shows a typical retention diagram for a series of alkanes and acetates; the isotherm changes at 140 °C with a sharp turn down at 171 °C; 171 °C is our measured PVF2 melting temperature from the IGC method. This melting temperature is in good agreement with the melting temperature reported by the supplier of PVF2 used in this work (Aldrich Chemical Co.) and with others reported in the literature.[14] We should note, however, that our data at 120 °C are higher than expected for alkanes only; this is due to an experimental error. The break in the lines is in agreement with previous retention diagrams obtained on different semicrystalline polymers.[3,13,14]

Degree of Crystallinity of PVF2. The IGC method has been used by previous investigators[3,14,30] to measure the crystallinity of polymers. In this paper we would like to demonstrate that the IGC method, with careful data analysis, is a practical, reliable, and fast method of obtaining detailed information about the degree of crystallinity of polymers. In the past, the degree of crystallinity of PVF2 was reported as a wide range over a range of

Table V
PVF2-Solute Interaction Coefficients (χ_{12}) at Various Temperatures

probe	80 °C	100 °C	120 °C	140 °C	160 °C	180 °C	200 °C	220 °C
pentane	1.44	1.32	1.38	1.36	0.99			
hexane	2.35	2.06	1.79	1.71	1.77			
heptane	2.75	2.42	2.15	2.04	2.19			
octane	3.27	2.92	2.58	2.53	2.63	2.15	1.89	1.72
nonane	3.75	3.39	3.04	3.08	3.04	2.05	1.91	1.65
decane	4.04	3.65	3.33	3.45	3.53	2.16	1.95	1.63
undecane	3.89	4.22	3.60	3.66	3.34	2.32	2.11	1.82
dodecane	4.49	4.42	3.73	4.07	3.06	2.65	2.39	2.06
benzene	1.41	1.11	0.85	0.78	0.87			
toluene	1.29	1.15	1.00	0.81	0.90			
methylene chloride	3.83	2.90	2.21	1.81	1.80			
carbon tetrachloride	2.32	1.99	1.73	1.56	1.70			
tetrahydrofuran	0.44	0.21	0.04					
dioxane	0.07	−0.05	−0.08					
acetone	−0.30	−0.39	−0.37					
methyl ethyl ketone	−0.03	−0.08	−0.07					
methyl acetate	0.01	0.03	−0.02					
ethyl acetate	−0.03	−0.07	−0.09					
propyl acetate	0.33	0.16	0.08					
n-butyl acetate	0.55	0.38	0.27	0.11	0.19			

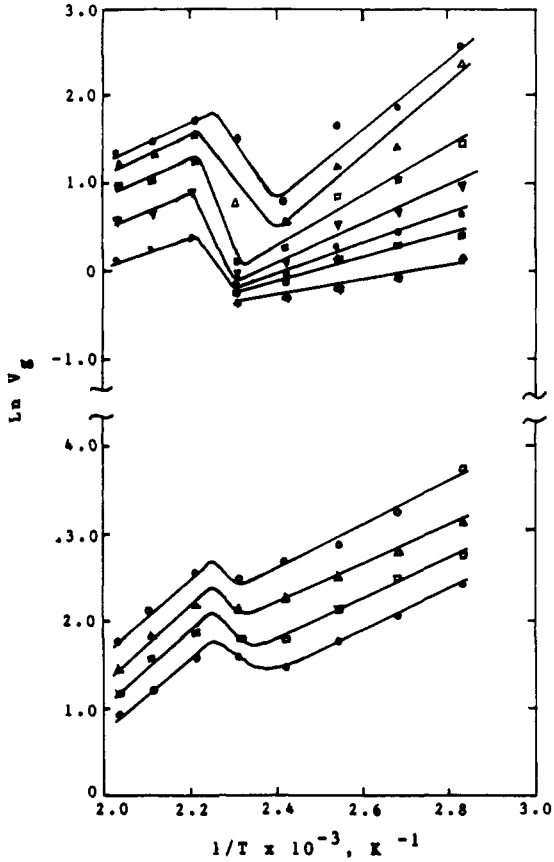

Figure 6. Retention diagrams of PVF2. Retention volumes vs $1/T$ for: Lower: acetates series, ●, methyl; □, ethyl; △, propyl; ○, butyl acetate. Upper: alkanes series, ●, hexane; ■, heptane; ●, octane, ▼, nonane; □, decane; △, undecane; ○, dodecane.

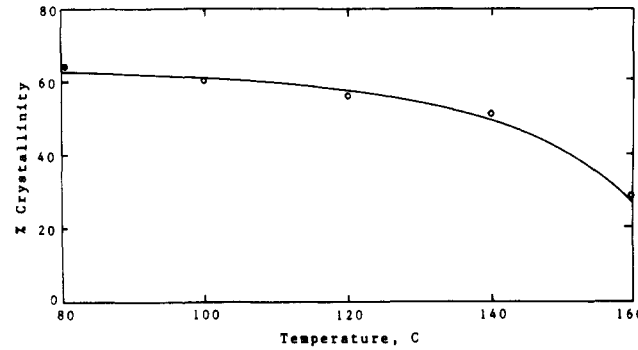

Figure 7. Dependence of degree of PVF2 crystallinity on temperature.

temperatures (50–68%, ref 31–33). In this work, the degree of crystallinity of PVF2 is obtained at an individual temperature, and we believe that this is the first detailed information on PVF2 crystallinity to be reported. Table III shows the percent crystallinity of PVF2 over the temperature range 80–160 °C. The *n*-acetate series was selected as probes to measure the crystallinity because acetates have more interaction than other probes with PVF2. Thus, in this case, corrected specific retention volumes of acetates are more dependable than the V_{g_b} of other probes. Furthermore, a series of four acetates was selected to check the validity of our results. The degree of crystallinity was calculated from the retention diagram (Figure 6); the straight line above the melting point was extrapolated to the crystalline region. When the extrapolated line met the desired temperature, two readings were taken, $V_{g_{amorph}}$ and $V_{g_{sample}}$; then, by use of eq 18, the crys-

$$\% X_c = 100[1 - (V_{g_{sample}}/V_{g_{amorph}})] \quad (18)$$

tallinity was calculated. The percent crystallinity listed in Table III measured by using four acetates at an independent temperature shows a good agreement among the acetate series. The percent crystallinity was averaged at each temperature; the crystallinity ranged from 64.1% at 80 °C to 28.7% at 160 °C. The error in the averaged crystallinity values is better than 3%. At 160 °C, PVF2 starts to melt, and the crystallinity was sharply reduced to 28.7% and then reduced to zero at 171 °C, where PVF2 is completely melted. Figure 7 shows the relationship of the percent crystallinity of PVF2 with temperature; similar relationship were obtained previously on a semicrystalline polypropylene[13] by using the IGC method. The crystallinity values were incorporated in eq 9 to calculate the specific volume at each temperature (Table II).

Interaction and Other Thermodynamic Parameters. PVF2–solute interaction parameters were calculated according to eq 3, below and above the PVF2 melting temperature. Table V shows χ_{12} for 20 probes as a function of temperature below the PVF2 melting temperature and for only the alkane series above the PVF2 melting temperature, because Antoine equation constants for the remaining probes are not available above 180 °C. Previously, IGC researchers considered the region between the melting and the glass transition temperatures to be nonequilibrium

Table VI
Weight Fraction Activity Coefficients, Partial Molar Heat of Mixing, and Partial Molar Free Energy of Mixing of PVF2-Solute System at Various Temperatures

	Ω_1^∞				ΔG_1^∞, kcal/mol		
probe	180 °C	200 °C	220 °C	ΔH_1^∞, kcal/mol (200 °C)	180 °C	200 °C	220 °C
octane	71.83	58.82	50.83	3.76	3.85	3.83	3.85
nonane	62.55	55.97	44.58	3.81	3.72	3.78	3.72
decane	67.55	56.37	42.56	5.01	3.79	3.79	3.68
undecane	77.61	63.99	49.81	4.81	3.92	3.91	3.83
dodecane	105.96	83.62	61.45	5.91	4.20	4.16	4.04

Table VII
Partial Molar Heat of Sorption (ΔH_1^s) and Partial Molar Free Energy of Sorption (ΔG_1^s) of PVF2-Solute Systems at 200 °C

probe	ΔH_1^s, kcal/mol	ΔG_1^s, kcal/mol
octane	−2.63	5.26
nonane	−3.69	4.73
decane	−3.25	4.28
undecane	−4.33	3.93
dodecane	−4.11	3.73
methyl acetate	−6.81	3.35
ethyl acetate	−8.31	3.16
propyl acetate	−8.57	2.78
n-butyl acetate	−8.58	2.36

sorption region with no justification other than the contribution of the surface adsorption of the probe to V_g. However, since our V_{g_b} corresponds only to the absorption of the probe in the amorphous layer, one would assume that an equilibrium is established between the probe and the amorphous region. We already eliminated the mass of the crystalline part of PVF2 by eq 17, and the mass of only the amorphous part is incorporated in the calculation of V_{g_b} and χ_{12}. Our results show that the acetate series are much better solvents for PVF2 than other solvents used in this work. In addition, methyl and ethyl acetates are the best solvents for PVF2. However, the alkane series showed larger interaction coefficients than other probes, suggesting that alkanes are nonsolvent probes. In support of our observation, endothermic excess heats of mixing ($\Delta H_1^\infty = 3 \rightarrow 6$ kcal/mol) for alkanes were observed. These nonsolvents probes have V_{g_b} values of less than 6 mL/g at 200 °C. χ_{12} for alkanes did not show any considerable change with temperature below PVF2 melting temperature; however, above the melting temperature, a considerable decrease in χ_{12} was observed. χ_{12} for the acetate series and carbonyl-containing compounds above 120 C were not calculated due to the lack of Antoine constants, except for *n*-butyl acetate. Our observed solubility for PVF2–solute system is in good agreement with earlier reported data.[14]

We observed lower values of χ_{12} above the PVF2 melting temperature than below the melting temperature (Table V). Since χ_{12} is a function of the inverse of vapor pressure and molar volume of probes, our observation is in good agreement with the theoretical prediction of χ_{12} vs temperature and with the results of other workers.[34-36]

The thermodynamic sorption parameters, ΔG_1^s, ΔH_1^s, and $T\Delta S_1^s$ in kcal/mol for the alkanes and acetates series at 200 °C were calculated (Table VII). The sorption process involves the transfer of the solute molecules from the vapor phase into the amorphous part of PVF2. This process strongly depended on the PVF2–solute interaction, and therefore the heat of sorption associated with this process depends on the interaction too. Above the PVF2 melting temperature, we focused on the interaction of only two series with PVF2, alkanes and acetates: the latter has been found to have a strong interaction with PVF2. To have a better understanding of this interaction, we plotted

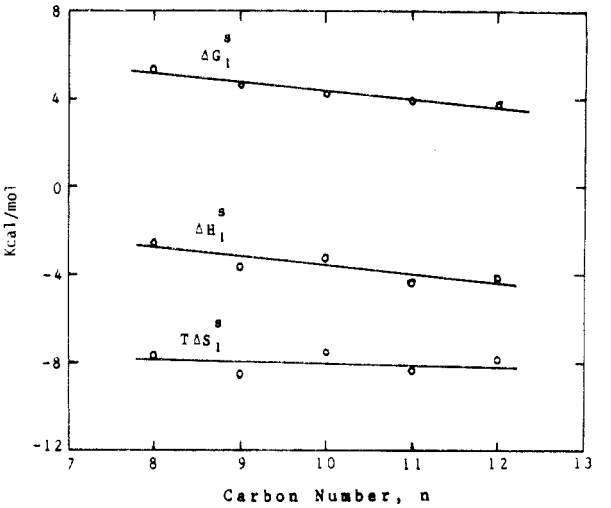

Figure 8. Family plot for *n*-alkanes; ΔG_1^s, ΔH_1^s, and $T\Delta S_1^s$ vs number of carbons at 200 °C.

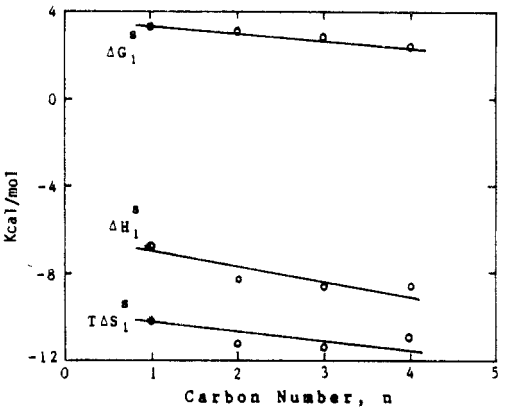

Figure 9. Family plot for acetates: ΔG_1^s, ΔH_1^s, and $T\Delta S_1^s$ vs number of carbons at 200 °C.

our calculated sorption parameters in a family type plot. Figures 8 and 9 show a linear relationship between the thermodynamic sorption parameters and the number of carbon of the alkane and acetates series. The slopes of these lines may be meaningful to obtaining the contribution of the CH_2 group in both series to ΔH_1^s, ΔG_1^s, and $T\Delta S_1^s$, thus allowing a better understanding of the interaction of the CH_2 group with PVF2 sites. Since there is no expected formation of hydrogen bonding between the cis or gauch forms of PVF2 and solutes of both series, the attraction forces must be a van der Waals (dispersive) type forces. The contribution of CH_2 of alkanes (slope obtained from Figure 8) to the partial molar heat of sorption was found to be exothermic and is −0.44 kcal/mol, while the contribution of the CH_2 group of acetates to ΔH_1^s is more exothermic, −0.73 kcal/mol. It is clear that the slope obtained from the acetate series is more exothermic than that obtained from the alkane series, simply because there are two interaction sites in the acetates, CH_2 and C=O groups. Thus one would obtain the C=O group contribution to the

Table VIII
C=O and CH_2 Group Contributions to the ΔH_1^s, ΔG_1^s, and $T\Delta S_1^s$ in kcal/mol

group	ΔH_1^s	ΔG_1^s	$T\Delta S_1^s$
alkanes, CH_2	−0.44	−0.41	−0.06
acetates, CH_2	−0.73	−0.34	−0.46
acetates, C=O	−0.29	0.07	−0.40

ΔH_1^s by subtracting the alkanes slope from the acetates slope; a value of −0.31 kcal/mol was obtained. Evidently the nature of the dispersive attraction forces between the solute and PVF2 has an influence on the sorption process. Alkanes have weaker dispersive attraction with PVF2 backbone than acetates; however, our calculations showed that an individual CH_2 group has considerable interaction with PVF2 (presumably with the fluorine atom).

Similar calculations have been made for the contribution of CH_2 of alkanes and acetates to the partial molar free energy ΔG_1^s and to the sorption entropy $T\Delta S_1^s$; the results are shown in Table VIII.

Conclusions

We have shown in this article that the inverse gas chromatography (IGC) method can be fast, reliable, and versatile as a method for polymer characterization. However, to obtain a meaningful value for specific retention volumes, heat of mixing, interaction coefficients, and many other thermodynamic quantities, many corrections have to be carried out to compensate for the contribution of the solid support, the carrier-gas flow rate, and the loading of the polymer. Below the melting point of PVF2, retention volumes of 20 probes were obtained as a combination of two contributions, due to the adsorption on the crystalline surfaces and the absorption by the amorphous part of the polymer. A procedure was established to eliminate the contribution of the surface adsorption to the retention volumes of solutes, allowing the calculation of meaningful interaction parameters for PVF2–solute systems below and above the PVF2 melting temperature. Our results showed that acetates and carbonyl-containing solutes are better solvents than nonpolar alkanes. The degree of crystallinity and specific volumes of PVF2 below its melting temperature were calculated from the obtained retention diagram of acetates. Crystallinity ranged between 64% and 29% over the temperature range 80–160 °C.

The interaction mechanism of PVF2–solute system was explained via explained on the basis of the calculated thermodynamic parameters. $\Delta \bar{H}_1^\infty$, ΔG_1^∞, ΔH_1^s, ΔG_1^s, and $T\Delta S_1^s$ for the mixing and the sorption processes of the probes were obtained, and the contribution of CH_2 and C=O in alkanes and acetates to these parameters was calculated. The CH_2 group generally has more interaction with PVF2 backbone than the C=O group, which demonstrates that the dispersive type attraction forces occurred between PVF2 and CH_2 groups in solutes is stronger than that between PVF2 and C=O groups.

Acknowledgment. We are grateful to Monsanto Co. for supporting this work and for providing a postdoctoral fellowship for C.-T.C. Thanks are also due to Drs. P. Munk (University of Texas at Austin) and El-Hibri (Amoco Corp.) for allowing us to use their IGC software.

Registry No. PVDF, 24937-79-9; pentane, 109-66-0; hexane, 110-54-3; heptane, 142-82-5; octane, 111-65-9; nonane, 111-84-2; decane, 124-18-5; undecane, 1120-21-4; dodecane, 112-40-3; benzene, 71-43-2; toluene, 108-88-3; methylene chloride, 75-09-2; carbon tetrachloride, 56-23-5; tetrahydrofuran, 109-99-9; dioxane, 123-91-1; acetone, 67-64-1; methyl ester ketone, 78-93-3; methyl acetate, 79-20-9; ethyl acetate, 141-78-6; propyl acetate, 109-60-4; butyl acetate, 123-86-4.

References and Notes

(1) Al-Saigh, Z. Y.; Munk, P. *Macromolecules* **1984**, *17*, 803.
(2) Card, T. W.; Al-Saigh, Z. Y.; Munk, P. *Macromolecules* **1985**, *18*, 1030.
(3) Smidsrod, O.; Guillet, J. E. *Macromolecules* **1969**, *2*, 272.
(4) Gray, D. G.; Guillet, J. E. *Macromolecules* **1974**, *7*, 244.
(5) Gray, D. G.; Guillet, J. E. *Macromolecules* **1971**, *4*, 129.
(6) Braun, J. M.; Guillet, J. E. *Macromolecules* **1975**, *8*, 882.
(7) Deshpande, D. D.; Tyagi, O. S. *Macromolecules* **1978**, *11*, 746.
(8) Card, T. W.; Al-Saigh, Z. Y.; Munk, P. *J. Chromatogr.* **1984**, *301*, 261.
(9) Munk,, P.; Al-Saigh, Z. Y.; Card, T. W. *Macromolecules* **1985**, *18*, 2196.
(10) Munk, P.; Card, T. W.; Hattam, P.; El-Hibri, M. J.; Al-Saigh, Z. Y. *Macromolecules* **1987**, *20*, 1278.
(11) Braun, J. M.; Guillet, J. E. *Macromolecules* **1977**, *10*, 101.
(12) We have noted that this procedure could contribute to a large error if the carrier gas is helium; see ref 8.
(13) Alishoev, V. R.; Berezkin, V. G.; Melnikova, Y. V. *Russ. J. Phys. Chem.* **1965**, *39*, 105.
(14) DiPaola-Baranyi, G.; Fletcher, S. J.; Degre, P. *Macromolecules* **1982**, *15*, 885.
(15) Kawai, H. *Jpn. J. Appl. Phys.* **1969**, *8*, 975.
(16) Littlewood, A. B.; Phillips, C. S. G.; Price, D. T. *J. Chem. Soc.* **1955**, 1480.
(17) Dreisbach, R. R. *Adv. Chem. Ser.* **1955**, *No. 15*; **1959**, *No. 22*; **1961**, *No. 29*.
(18) McGlashan, M. L.; Potter, D. J. B. *Proc. R. Soc. London, Ser. A* **1967**, *267*, 478.
(19) Van Krevelen, D. W. *Properties of Polymers*; Elsevier New York, 1972.
(20) Lipson, J. E. G.; Guillet, J. E. *Developments in Polymer Characterization—3*; Dawkins, J. V., Ed.; Applied Science Publishers: England, 1980; p 33.
(21) Patterson, D.; Tewari, Y. B.; Schreiber, H. P.; Guillet, J. E. *Macromolecules* **1971**, *4*, 356.
(22) Everett, D. H. *Trans. Faraday Soc.* **1965**, 1637.
(23) The molecular weight of PVF2 was kindly measured by the analytical section of Union Carbide Corp., Technical Center, South Charleston, WV.
(24) Braun, J. M.; Cutajar, M.; Guillet, J. E. *Macromolecules* **1977**, *10*, 864.
(25) Aue, W. A.; Hasting, C. R.; Kapila, S. J. *J. Chromatogr.* **1973**, *77*, 299.
(26) Lamb, R. J.; Purnell, J. H.; Williams, P. S.; Harbison, M. W.; Martire, D. E. *J. Chromatogr.* **1978**, *155*, 233.
(27) Martin, R. L. *Anal. Chem.* **1961**, *33*, 347.
(28) El-Hibri, M. J.; Munk, P. *Polym. Prepr. (Am. Chem. Soc., Div. Polym. Chem.)* **1987**, *28*, 262.
(29) Galin, M.; Maslinko, L. *Macromolecules* **1985**, *18*, 2192.
(30) Courval, G.; Gray, D. G. *Macromolecules* **1975**, *8*, 326.
(31) Paul, D. R.; Altamirano, J. O. *Adv. Chem. Ser.* **1975**, *142*, 371.
(32) Thompson, D. C.; Barney, A. L. *Encycl. Polym. Sci. Technol.* **1971**, *14*, 600.
(33) El-Hibri, M. J.; Paul, D. R. *J. Appl. Polym. Sci.* **1986**, *31*, 2533.
(34) Sanetra, R.; Kolarz, B. N.; Wlochowicz, A. *Polymer* **1987**, *28*, 1753.
(35) Fernandez-Berridi, M. J.; Guzman, G. M.; Irvin, J. J.; Elorza, J. M. *Polymer* **1983**, *24*, 417.
(36) Equiazobal, J. I.; Fernandez-Berridi, M. J.; Irvin, J. J.; Elorza, J. M. *Polym. Bull.* **1985**, *13*, 463.